Preferred citation: K.J. Niskanan. Distribution of fibre orientations in paper. In **Fundamentals of Papermaking**, *Trans. of the IXth Fund. Res. Symp. Cambridge, 1989*, (C.F. Baker & V. Punton, eds), pp 275–308, FRC, Manchester, 2018. DOI: 10.15376/frc.1989.1.275.

DISTRIBUTION OF FIBRE ORIENTATIONS IN PAPER

K. J. Niskanen
Paper Science Center, The Finnish Pulp and Paper Research Institute,
P.O.B. 136, SF-00101 Helsinki, Finland

ABSTRACT

During web formation, the difference between the speed of the pulp suspension and that of the wire gives rise to a shear force that orients fibres preferentially along the machine direction. This has been known for a long time. It is less clear, however, how the distribution of fibre orientations is actually related to the conditions of web formation and to the properties of papermaking fibres. We have studied this question using simple theoretical models and experimental data including image analysis results.

We find that fibre-to-fibre interactions determine how much individual fibres are rotated by the oriented shear field. In this way the fibre orientation distribution obtained for a given speed difference depends on the pulp properties. On the other hand, the turbulence of the pulp flow seems to be the mechanism through which the conditions of web formation affect fibre orientation. In particular, we suggest that the onset of shear-induced turbulence in the suspension flow determines the maximum fibre orientation anisotropy that can be achieved.

The model calculations show that the distribution of fibre orientations cannot be represented in terms of a simple functional form with only one adjustable parameter. The shape of the distribution depends on the fibre properties, and especially the wet fibre flexibility. In paper the orientation distribution of curly fibres is quite different from that of straight fibres. On the other hand, no difference in the distribution is observed if long and short fibre are examined separately.

1. INTRODUCTION

In the web formation process (1) there are several factors that affect the distribution of fibre orientations in paper: the suspension acceleration in the slice channel of the headbox, the difference between the speed of the suspension and that of the wire, drainage forces and nonuniform suspension flow (or "turbulence") on the wire. Moreover, wet web draws may change fibre orientation. Under given process conditions, the orientation distribution may also depend on the properties of individual fibres and of their suspension. In this paper we shall study the significance of these factors on the distribution of fibre orientations in paper made by the Fourdrinier process.

In paper making fibre orientation is controlled by means of the jet-to-wire speed difference. The speed difference induces an oriented shear field in the suspension that acts on the fibres and makes them orient preferentially along the machine direction. This has been well demonstrated in the literature, with the machine to cross direction tensile ratio R_T as a common measure of the anisotropy - see e.g. Schröder, Svensson and Österberg (2,3).

Typical behavior of the tensile ratio as a function of the jet-to-wire speed difference is illustrated in Fig. 1 a for various paper grades made on the Fourdrinier pilot machine at the Finnish Pulp and Paper Research Institute (FPPRI, cf. Appendix for details). When the jet velocity is close to that of the wire ($v_S \approx 0$) the shear velocity is small and hence paper anisotropy weak. If, on the other hand, the speed difference is made larger, the paper becomes more anisotropic but only up to a certain level. At large speed differences the tensile ratio is observed to be independent of the speed difference.

In addition to the tensile ratio we have in some cases measured the distribution of fibre orientations on the top and wire side surfaces of the paper sample by image analysis techniques (see the Appendix for details); results for the fine paper and LWC base paper are shown in Figs. 1 b and c, respectively. The orientation index R_N will be defined later (Eq. (9)), at this point it is sufficient to know that in principle R_N should be roughly equal to the tensile ratio R_T. This is indeed the case for the low basis weight LWC-base paper (Fig. 1 c) where no fibre orientation twosidedness was detected in the image analysis.

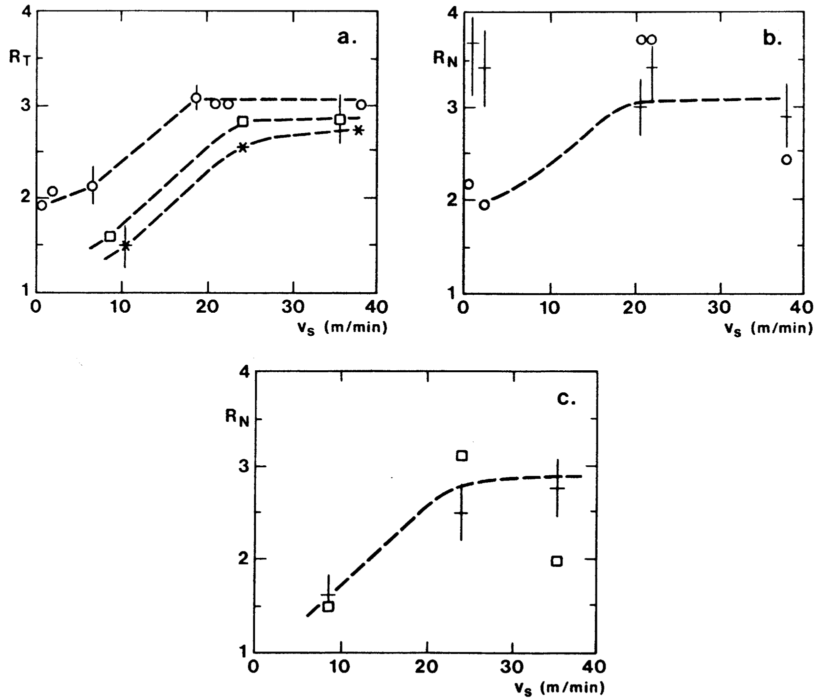

Fig 1. Tensile ratio R_T, a, and fibre orientation index R_N, Eq. (9), evaluated from the image analysis results, b and c, as a function of the suspension speed v_s relative to the wire for samples prepared on the FPPRI pilot machine. The dashed lines are drawn to guide the eye. The symbols are, a, ○ fine paper, □ LWC base paper and ✳ newsprint; ,b and c, ○ and □ the top side and the crosses the wire side of fine paper and LWC, respectively. Typical error margins are shown by the vertical bars, a, and by the size of the crosses, b and c.

In the fine paper case (Fig. 1 b) the image analysis results show significant twosidedness in fibre orientation. As only fibres on the surfaces were measured, it is not clear how well an average of the results would reflect the fibre orientation of the paper as a whole. Comparison with the tensile ratio suggests that the average orientation should be relatively close to that visible on the top side. In any case, the distribution of fibre orientations in the fine paper is quite different from that in the LWC base paper.

Since the total MD straining of the web was approximately the same in all three cases (cf. Appendix), most of the tensile ratio variation in Fig. 1 a must arise from fibre orientation. On the other hand, it is quite clear that some of the differences between different paper grades may be accounted for by variations in internal stress. The level of internal stresses depends on the shrinkage potential of the pulp (4) and therefore the contribution of internal stress to the tensile strength anisotropy could be successively lower for the fine paper, the LWC base paper and the newsprint, as also observed in the experiments.

In this connection we remark that wet strain has little significance in the distribution of fibre orientations (5). It is easy to show that if an isotropic fibre network is strained by ϵ %, then the fibre orientation index should be approximately equal to $R_N \approx 1 + 0.015 \cdot \epsilon$.

It is in general impossible to separate the effects of internal stresses and fibre orientation on paper anisotropy by means of measurements. We shall nevertheless use the tensile ratio as a measure of the fibre orientation anisotropy. In practice the tensile ratio R_T is still the most widely used measure of fibre orientation anisotropy.

In terms of Figs. 1, there are three questions we shall consider in this study. First, what determines the distribution of fibre orientations in the absence of the shear velocity (v_S=0)? According to Figs. 1, the minimum anisotropy could depend on pulp properties (wood-free vs. wood-containing) or process variables (e.g. machine speed 60 m/min vs. 80 m/min) or both.

Second, we would like to know how fast the anisotropy of fibre orientation increases as the jet-to-wire speed difference is increased, and third, we would like to determine the factors that control the saturation of fibre orientation. In other words, what is the speed difference beyond which the anisotropy no longer increases, and what is the fibre orientation anisotropy thus achieved? In the case of the FPPRI pilot machine all the paper grades studied appear to be quite similar in this respect.

It was clearly shown in the studies of Schröder, Svensson and Österberg (2,3) that the quality of paper formation is quite sensitive to the jet-to-wire speed difference. Good formation may be obtained if the speed difference is not too large whereas if the speed difference exceeds a certain limit, formation quality deteriorates rapidly.

It is interesting that upon increasing the speed difference the fibre orientation anisotropy levels off at about the same point where the formation index starts to increase. This observation suggests that the poor formation quality and the saturation of the fibre orientation anisotropy are both caused by a change in the flow state of the pulp suspension. In particular, one could think that if the shear field during web formation is too large "turbulence" could dominate the fibre network structure of paper.

In this paper we report qualitative model calculations of the physical mechanisms of fibre orientation aimed at understanding how the distribution of fibre orientations in paper depends on the papermaking process and on the pulp properties. The model predictions are used to analyse experimental results including data based on the image analysis of stained fibres in sheets prepared on the FPPRI Fourdrinier pilot machine.

2. ORIENTATION BY LAMINAR SHEAR

We shall start by considering the behavior of fibres in the shear field induced by the speed difference between the jet and the wire. The suspension flow is assumed to be laminar so that no "turbulence" or other irregularities are present. Also, the suspension consistency is assumed to be low enough so that fibre-to-fibre interactions in the suspension phase can be ignored.

2.1. Model for laminar shear

In principle, one could attempt to find the precise mathematical expression for the distribution of fibre orientations by solving the hydrodynamic equations of motion of the pulp suspension. As early as the 1920s, Jeffery (6) studied the motion of ellipsoidal particles in a viscous fluid. His results were later applied to the case of stiff rods in sheared suspensions by Mason et. al. (7). In experiments they found that the motion of glass fibres was indeed in good agreement with the predictions of Jeffery's theory.

On the other hand, Jeffery's equations of motion are complicated. Even under very strong simplifying assumptions it does not appear possible to derive a closed form equation to describe the real distribution of fibre orientations in paper. We will therefore solve the problem approximately and derive a qualitative solution. This solution can then be applied to discuss the effects of process variables and pulp properties.

Let us consider the case of a low consistency of straight stiff fibres flowing a regular laminar shear velocity field. Assume also that the fibres in the suspension have no preferential orientation, i.e. ignore jet orientation. The nonlaminar flow and the jet fibre orientation will be discussed in later sections.

During web formation one end of each fibre first comes down on the filtered fibre mat (on the wire during initial drainage) while the other end is still floating free in the suspension. This stage is shown schematically in Fig. 2 as seen directly from above. The direction of the fibre with respect to the direction of the suspension flow (relative to wire) is given by the angle ϕ.

The stiff fibre will have to rotate around its fixed end along the flow. The fibre mat counteracts the axial stress that the fluid exerts on the fibre. Thus the flow slips on the fibre surface in the direction of the fibre axis and the net force exerted on the fibre is perpendicular to the direction of the fibre. The rotation of the fibre should be most rapid when ϕ =

$\pi/2$ and, on the other hand, the fibre should not rotate at all if $\phi = \pm\pi$ or $\phi = 0$. Also, the fibre should always rotate towards the value $\phi = 0$ and away from $\phi = \pm\pi$. This means that if the fibre comes down "nose" (rather than "tail") first - so that initially $|\phi| > \pi/2$ - then after a certain while it will point in the cross-machine direction. Thus the shape of the distribution of fibre orientations may have some rather unexpected features as we shall see in section 4.2.

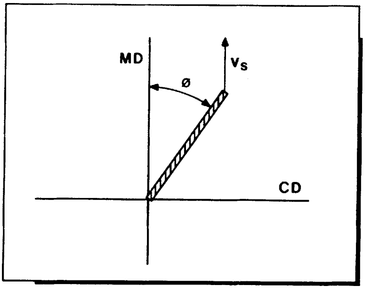

Fig. 2. Schematic illustration of a fibre during the drainage phase anchored to the wire from the end located at the origin. Orientation relative to machine direction is given by the angle ϕ.

Since the fibre mass density is relatively close to that of the suspension we assume that inertial effects can be ignored. Then the simplest assumption for the rotation of the fibre is given by writing the speed of rotation $d\phi/dt$ in the form

$$d\phi/dt = -\Gamma \cdot v_S \cdot \sin(\phi) \quad (1)$$

where Γ is a parameter and v_S characterises the speed of the suspension relative to the wire.

The shape of the velocity profile of the suspension close to the wire should, in principle, be taken in to account by treating v_S as a function of the z-directional orientation of the fibre. Also, in reality the time evolution of the z-directional orientation couples to the angle ϕ which would further complicate the mathematics. We shall ignore these complications.

We emphasize that Eq. (1) is nothing more than a simple mathematical expression that, as we shall show, can be used to describe qualitatively the physical processes that give rise to fibre orientation. We assume that the model parameters can be adjusted appropriately so that the right hand side of Eq. (1) reasonably well represents the average behaviour of fibres in the oriented shear field.

The solution of Eq. (1) is of the form

$$\tan(\phi/2) = C \tan(\phi_o/2) \tag{2}$$

where

$$C = \exp(-\beta \cdot v_s) \tag{3}$$

and ϕ_o is the initial orientation of the fibre when one end of is anchored to the filtered fibre mat. The parameter β is given by $\beta = \Gamma t_z$ where t_z is the time it takes for the fibre to stop rotating and land on the wire. More generally, β tells how much a fibre is able to rotate in the shear field.

Next we observe that the initial distribution of fibre orientations in the suspension, $g(\phi_o)$, and the final distribution in the paper, $f(\phi)$, are basically related to one another through an equation of the form $f(\phi)d\phi = g(\phi_o)d\phi_o$. However, in the final paper sheet it is not possible to tell which way the fibres have landed, and therefore the orientation distribution has to satisfy the requirement $f(\phi+\pi) = f(\phi)$. Thus the initial and final distribution are related by

$$f(\phi)d\phi = [g(\phi_-)d\phi_- + g(\phi_+)d\phi_+]/2 \tag{4}$$

where $\phi_o = \phi_-$ and ϕ_+ are the solutions of Eq. (2) corresponding to ϕ and $\phi+\pi$ respectively:

$$\cos \phi_\pm = [\pm\cos(\phi) + p]/[\pm p\cdot\cos(\phi) + 1] \tag{5}$$

where

$$p = \tanh(\beta \cdot v_s) \tag{6}$$

From preceding equations it follows that if the initial values ϕ_o are isotropically distributed, $g(\phi_o) = 1/\pi$, then fibre orientations in paper obey the elliptic distribution

$$f(\phi) = f_E(\phi,q) = (1/\pi)\cdot\frac{(1-q^2)}{[1+q^2-2\cdot q\cdot\cos(2\phi)]} \tag{7}$$

where

$$q = p^2 = \tanh^2(\beta\cdot v_S) \tag{8}$$

Eqs. (7) and (8) define a model for the distribution of fibre orientations in Fourdrinier-made paper under the simplifying assumptions that the stiff fibres rotate independently of one another, that the suspension flow is laminar, and that there is no preferred fibre orientation in the suspension prior to filtration.

In order to characterise the anisotropy of fibre orientations we evaluate the orientation index R_N already used in Figs. 1 b and c as being the network theory (8) prediction for the machine to cross direction ratio of the elastic moduli:

$$R_N = [6+4\cdot a_1+a_2]/[6-4\cdot a_1+a_2] \tag{9}$$

R_N is a reasonable measure of the fibre orientation contribution to the mechanical anisotropy, both elastic and tensile strength ratio (9). The coefficients a_1 and a_2 are those of the Fourier expansion

$$f(\phi) = (1/\pi)\cdot\{\ 1 + \sum_{n=1}^{\infty} a_n\cdot\cos(2\cdot n\cdot\phi)\ \} \tag{10}$$

which can always be employed to represent the distribution of fibre orientations in paper (assuming of course that on the average the fibres are aligned along the machine direction $\phi=0$). In the case of the elliptic distribution function a_n is given by

$$a_n = 2\cdot q^n\ . \tag{11}$$

In Fig. 3 we show that the elliptic distribution $f_E(\phi)$, Eqs. (7) and (8), leads to an orientation index R_N that grows at an increasing rate as the difference between the speed of the suspension and that of the wire grows. The qualitative nature of the model does not allow us to calculate a value for the parameter β but, instead, β can be used as an adjustable parameter. In the figure, β has been arbitrarily chosen to be β = 0.05 min/m.

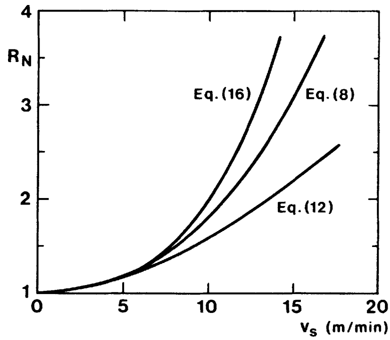

Fig. 3. Orientation index R_N, Eq. (9), as a function of the suspension speed v_S evaluated for the elliptic models defined by Eq. (8) and Eq. (12), and for the von Mises model, Eq. (16). The model parameters are β=0.05 min/m, v_Z=10 m/min, and K is given by Eq. (17).

We believe that the elliptical distribution function $f_E(\phi)$, Eqs. (7) and (8), qualitatively describes the effect of the laminar shear field on the distribution of fibre orientations in paper. We shall use this model in the subsequent sections in the study of the effects on fibre orientation of drainage, jet orientation, turbulence and pulp properties. First, however, we shall briefly consider two other simple models for the fibre orientation distribution.

2.2. Other simple models

First, we point out that an elliptic distribution of fibre orientations was also derived by Ryti et. al. (10) in connection with an oblique sheet mould. In this mould the fibre orientation anisotropy is controlled by the angle of suspension flow relative to a horizontal wire. If the flow is vertical no anisotropy is generated in the sheet, whereas if the flow approaches horizontal then the sheet becomes strongly anisotropic.

Ryti et. al. derived their model starting with the assumption that every fibre becomes oriented in the direction of its projection in the plane perpendicular to the flow direction. The distribution thus obtained differs from our model only in the orientation parameter q. If the results of Ryti et. al. are transformed to the Fourdrinier case it is found that instead of Eq. (8) q is given by

$$q = \tan^2\{0.5\cdot\arctan(v_S/v_Z)\} \tag{12}$$

where v_Z is the vertical drainage speed through the wire.

The model derived by Ryti et. al. is thus quite similar to the one we derived above. In particular, if the suspension speed is close to that of the wire, $v_S \approx 0$, we find that Eq. (8) and (12) give, respectively,

$$q \approx (\beta\cdot v_S)^2 \tag{13}$$

and

$$q \approx (v_S/2\cdot v_Z)^2 \tag{14}$$

The two expressions are equal if

$$v_Z = (2\cdot\beta)^{-1} \tag{15}$$

If β = 0.05 min/m then according to Eq. (15) v_Z = 10 m/min. The curve thus obtained for the orientation index R_N is also shown in Fig. 3. It is seen that Eq. (12) is gives qualitatively the same behavior for R_N as Eq. (8), but large deviations do arise as v_S increases.

The distribution of fibre orientations in paper is often described by means of the von Mises distribution of the form

$$f(\phi) = f_M(\phi,K) = \exp[K\cdot\cos(2\cdot\phi)]/I(K) \tag{16}$$

where I(K) is the normalization constant. This is the periodic analog of the ordinary Gaussian distribution (9).

We are not aware of any microscopic motivation for the von Mises distribution. On the basis of statistical mechanics one could argue that the potential energy related to the rotational degrees of freedom in the MD-CD-plane of a fibre should in the simplest case be of the form $K \cdot \cos(2\phi)$ and therefore $f(\phi)$ should be of the von Mises type. However, it is difficult to say what the value of the parameter K should be as a function of the speed of the suspension relative to that of the wire, v_S.

If we assume, quite arbitrarily, that K is such that for small v_S the von Mises model, Eq. (16), gives the same values for the orientation index R_N as the elliptical model, Eqs. (7) and (8), we find that K should be given by

$$K = 2 \cdot (\beta \cdot v_S)^2 \tag{17}$$

It can be seen from Fig. 3 that the von Mises distribution gives a stronger curvature to the orientation index as a function of the suspension speed than the elliptical models.

The discussion has shown that the simple fibre orientation models give quantitatively quite different results when the anisotropy of fibre orientation is large. This is expected since drastic simplifications are necessary if any model at all is to be obtained. On the other hand, the results above also show that qualitatively all three models look alike.

2.3. Fibre orientation in the jet stream

We consider next what happens if fibres are oriented in the jet stream. It is quite clear that any orientation distribution that may exist in the jet vanishes very rapidly as the jet lands on the wire. Therefore, the effect of jet orientation should be visible mainly on the wire side of paper.

In the jet stream fibres are oriented preferentially along the machine direction when the suspension flow accelerates in the converging slice channel (12). We assume for simplicity that the cross-sectional area of the channel decreases linearly as a function of the distance from the lip. If, in addition, the suspension flow in the headbox is assumed to be laminar, then one can show that an elliptic distribution of fibre orientations is generated in the jet stream (13).

In other words, the distribution in the jet, $g(\phi)$, is approximately of the form defined in Eq. (7), $g(\phi) = f_E(\phi,q_j)$. It is easy to show that the elliptic parameter q_j is in this case given by

$$q_j = (k-1)/(k+1) \tag{18}$$

where $k = (A_1/A_2)^{\frac{1}{2}}$, and A_1 and A_2 are the cross-sectional areas of the entrance and exit of the converging slice channel.

The elliptic distribution of fibre orientations in the jet is again only an approximation. The suspension flow in the headbox is turbulent, and therefore the fibre orientation anisotropy tends to be weaker than Eq. (18) predicts. As the jet emerges from the lip the decreasing pressure causes a reduction in the fibre orientation anisotropy of the top and bottom layers of the stream (14). On the wire, turbulence and other flow disturbances rapidly destroy the fibre orientation anisotropy of the suspension.

In any case, let us assume that in the jet - and thus in the suspension during initial drainage - there is an anisotropic distribution of fibre orientations $g(\phi)$. Then it follows from Eqs. (4) and (5) that the corresponding distribution of fibre orientations in paper, $f(\phi)$, is given by

$$f(\phi) = \frac{1-p^2}{2}\cdot\left\{\frac{g(\phi_+)}{1+p^2-2p\cdot\cos\phi} + \frac{g(\phi_-)}{1+p^2+2p\cdot\cos\phi}\right\} \tag{19}$$

where $\phi o = \phi_{\pm}$ is given by Eq. (4) and $p = q^{\frac{1}{2}} = \tanh[\beta(v_s)]$ by Eq.(8).

The distribution function $f(\phi)$ defined by Eq. (19) and the corresponding Fourier coefficients can be evaluated numerically for any given initial distribution $g(\phi_o)$. Fig. 4 shows a typical example of how the jet fibre orientation affects the calculated orientation index R_N. We expect that the tensile ratio R_T should behave in a similar way.

The model calculation suggests, in particular, that the orientation index R_N is entirely determined by the jet fibre orientation for a range of small values of v_s. The corresponding speed range depends on the degree of fibre orientation in the jet (in our model on the parameter q_j). In fact, R_N goes through a minimum (although very weak) at a nozero v_S before it starts to increase with increasing suspension speed. Then the fibre orientation in paper is again controlled by the oriented shear field on the wire. The stronger the orientation in the jet the higher the suspension speed must be before its effect is observed. We note that the model is consistent with fact that in the fine paper case the wire side fibre orientation index R_N is independent of the suspension speed.

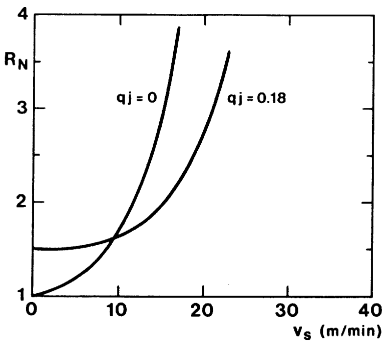

Fig. 4. Orientation index R_N, Eq. (9), as a function of the suspension speed v_S evaluated for the elliptical fibre orientation model (Eq. (19)) with jet fibre orientation (q_j=0.18) and without it (q_j=0); β=0.05 min/m.

In the experiments shown in Figs. 1 the wire side fibre orientation anisotropy appears to be strong in the fine paper pulp, whereas in the LWC pulp essentially no wire side fibre orientation is observed if the suspension speed v_S is small. It thus appears that strong jet fibre orientation has been generated in the headbox in the fine paper case but none in the LWC case. This difference is probably caused by the hydrodynamic properties of the papermaking pulps. Effects of fibre type and consistency on the jet fibre orientation were observed already by Wrist (12). In section 4.2. we shall argue that in fact fibre-to-fibre interactions are the most important single factor that control the extent to which fibres are oriented by a given oriented shear field.

Of course the jet fibre orientation also depends on the headbox type and the speed of the jet (headbox pressure). The FPPRI pilot machine is equipped with a rectifier roll headbox and it appears improbable that the difference in the fibre orientation anisotropy of the jet stream of the fine paper and the LWC suspensions is caused by the different machine speed in the experiments. In general, however, headbox pressure may well affect the jet fibre orientation through the turbulence generated in the headbox.

In conclusion, the model calculations show that if the suspension flow is laminar then the fibre orientation anisotropy - as observed e.g. in the tensile ratio - should grow with increasing rapidity as the difference between the speed of the suspension and that of the wire increases. The jet fibre orientation may give rise to an almost constant level of fibre orientation anisotropy for a range of small suspension speeds.

The laminar model is consistent with the experimental behaviour if the suspension speed is not too large. However, upon increasing suspension speed the fibre orientation anisotropy does not increase indefinetely but rather reaches a plateau. In the next section it is shown that nonlaminarity or turbulence of the suspension flow has to be included in the model to explain this.

3. NONLAMINAR SUSPENSION FLOW

The laminar fibre orientation model (Eqs. (7) and (8) or Eq. (19)) was derived assuming that all fibres would be alike in their properties and would experience the same average laminar shear field. In practice there are both systematic and random variations present in the properties of the pulp. More important, the suspension flow need not be laminar. In this section we shall show that by including flow disturbances in the model we can explain experimental observations.

In Figs. 5 we show experimental results (3) of Svensson and Österberg (a and b) and, for convenience, the data for the FFPRI pilot machine (c), already displayed in Fig. 1 a. The measured tensile ratio R_T is plotted as a function of the speed difference of the jet and the wire. The results in Fig. 5 a correspond to a Fourdrinier wire section equipped with table rolls whereas in the case of Fig. 5 b the first few rolls were replaced with four wet suction boxes. In the FPPRI wire section (Fig. 5 c) there were six foils followed by wet suction boxes. In Fig. 5 a the paper machine speed was varied, in Fig. 5 b the drainage rate and in Fig. 5 c pulp composition (cf. Appendix). In Fig. 5 b the paper machine speed was 180 m/min and in Figs. 5 a and b kraft pulp was used.

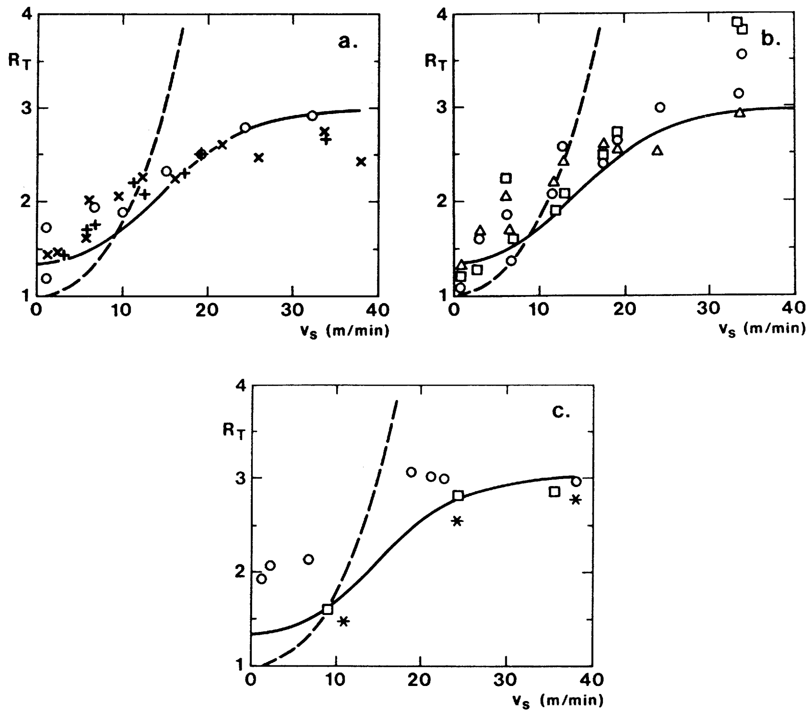

Fig 5. Tensile ratio R_T as a function of the suspension speed v_S relative to the wire, a and b, measured by Svensson and Österberg (3), and , c, the FPPRI pilot machine results already shown in Fig. 1 a. The symbols correspond to, a, paper machine speeds 120 m/min X , 180 m/min + , and 240 m/min O ; b, drainage rates low Δ , moderate O , and high □ ; and c, fine paper O , LWC base paper □ , and newsprint * . The solid and dashed lines show calculated orientation index R_N as explained in the text.

The dashed line in the Figs. 5 is the orientation index R_N calculated from the laminar fibre orientation model (Eqs. (7) and (8)) with β = 0.05 min/m. Clearly the simple model does not agree with experiments, not even if the value of β was changed. The same would hold for the other model equations considered in section 2.2. As shown in section 2.3., the jet fibre orientation may explain the anisotropy observed for small suspension speeds v_s relative to the wire speed, but not for large values of v_s.

Thus the laminar fibre orientation model is clearly inadequate to describe the fibre orientation anisotropy as a function of the suspension speed v_s relative to wire. We shall now show that the situation is greatly improved if disturbances in the suspension flow are taken into account. As a result, a fibre orientation model will be obtained that explains the experimental observations. The corresponding R_N is shown as the solid line in Figs. 5.

In the suspension flow systematic variations are always present which, in particular, give rise to the z-directional variation in the fibre orientation anisotropy. There are several sources for this. For example, the suspension speed v_s decays during drainage toward the wire speed, and thus the top side tends to be less oriented than than wire side. Because of wall friction the top and bottom layers of the jet stream have a lower speed than the interior layers. This, as well as the rapid dissipation of the fibre orientation induced in the headbox also induce twosidedness of fibre orientation. Systematic variations in the suspension flow cannot, however, explain the disagreement between the laminar model and experiments and we shall therefore not consider them any further.

Similarly, statistical variations in the pulp properties (e.g. fibre length and flexibility, local fibre concentration) are not expected to bring about any significant changes in the model predictions if they were included. In principle, this kind of random variations can be modelled by assigning a distribution of values to the parameter β of the laminar model. We shall ignore variations in pulp properties, too.

The suspension flow always has random components or some level of turbulence. This means that both the magnitude and direction of the oriented shear field varies in a random fashion. Turbulence is generated in the headbox and maintained during drainage by the drainage elements. In addition, turbulence is induced by the speed difference between the suspension and the wire (15).

In line with the preceding model calculations, we do not describe the flow disturbances in detail, but rather show their qualitative effect. For this purpose, we assign the suspension speed v_S a Gaussian distribution of mean half width σ and the flow direction another independent Gaussian distribution (of mean half width δ) around the machine direction. For simplicity, the effects of the jet fibre orientation are ignored. We emphasise that, on the one hand, one could choose some other form of statistical distribution but, on the other hand, that not be crucial for the qualitative effects we are looking for.

With the flow disturbances described by the two Gaussians, the elliptical distribution of fibre orientations $f_E(\phi,q(\beta\cdot v_S))$ (Eqs. (7) and (8)) is transformed into a new distribution which is best described by means of its Fourier coefficients a_n. It is easy to show that the original Eq. (11) is replaced by

$$a_n = 2\cdot\exp(-n^2\delta^2)\cdot\pi^{-\frac{1}{2}}\int_{-\infty}^{\infty}\exp(-x^2/\sigma^2)\tanh^{2n}[\beta(v_S-x)]dx \quad (20)$$

The Gaussian integral is conveniently evaluated by numerical methods.

When the "nonlaminar" fibre orientation model Eq. (20) is compared with experiments it is straightforward to adjust the three model parameters so that good agreement is obtained. This is illustrated in Fig. 6 where we show how the behaviour of the orientation index R_N changes with σ and δ. The curve denoted by I corresponds to the original laminar model, Eqs. (7) and (8), the curve II shows the effect of assigning a distribution of values to the suspension speed v_S and the curve III finally illustrates the effect of statistical variations in the suspension flow direction. As a result the experimental observations are quite well reproduced. The curve III is the same as the solid line in Figs. 5.

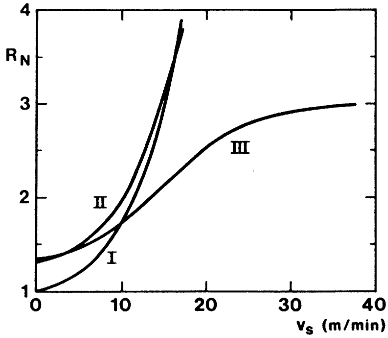

Fig. 6. Calculated fibre orientation index R_N, Eq. (20), with, I, β=0.05 min/m, σ=0 and δ=0; II, β=0.05 min/m, σ=10 m/min and δ=0; and III, β=0.10 min/m, σ=10 m/min and $\delta=\pi/3.2$.

Small adjustments in the model parameters could be made to improve the agreement with the individual data sets. For example, in the case of Fig. 5 c it would be quite reasonable that the value of β would vary with pulp type. Also the level of turbulence would probably depend on the configuration of drainage elements and therefore σ and δ should be adjusted separately for the data sets in Fig. 5 b.

More important than the quantitative agreement with the experiments are the qualitative implications of the model calculation. It is intuitively clear that variations in the suspension speed, σ, should be relevant when v_S is close to zero. If the average speed vanishes, v_S = 0, then any deviation from this average speed will give rise to a temporary orienting shear field, independent of the direction of the deviation. However, flow disturbances related to turbulent behaviour should be isotropically distributed and do not produce any machine directional fibre orientation in the paper. In that case the Gaussian distribution of flow directions in the model should be replaced by a uniform distribution, or δ set infinitely large, $\delta \to \infty$.

Thus, it appears that for $v_S \approx 0$ the fibre orientation anisotropy may be caused primarily by two factors: variations in the suspension speed or fibre orientation in the jet.

When the suspension speed is large the value of R_N is determined solely by the fluctuations in the flow direction. In papermaking millimetre scale turbulence is intentionally generated in order to prevent fibre flocculation. Even though fluctuations of greater length often arise unintentionally, it is clear that the fluctuations are smaller than the size of a typical macroscopic paper sheet. Thus the length scale of flow distrubances and turbulence is not relevant for the average anisotropy determined for a macroscopic paper sheet.

The intensity of turbulence varies from headbox to headbox and papermachine to papermachine, perhaps in the range of 1 to 10 m/min. In that respect the value of σ = 10 m/min used above is not unreasonable. However, in order to be able to reproduce the observed plateau in paper anisotropy ($R_T \approx 3$) at large values of v_s we have to choose quite large values of δ. For example, the value of $\delta = \pi/3.2$ would mean that the cross-directional flow velocity is frequently larger than the averege speed of the suspension relative to the wire. The magnitude of the flow disturbances suggested by the experimental values of R_T is thus quite large.

According to the experimental results shown in Figs. 5 the plateau in R_T is reached at about v_s = 20 m/min all cases studied. This suggests that there is a universal mechanism that gives rise to the plateau in paper anisotropy. From fluid mechanics we know that the shear stress imposed by an inert plate on a fluid flowing on it grows with the fluid speed, but if the fluid speed grows too large a boundary layer is created in which shear stress is dissipated by means of eddy currents and eventually fully developed turbulence. This mechanism has been confirmed experimentally (15).

In particular, it has been shown that at the papermaking consistencies a turbulent boundary layer is maintained if the pulp suspension flows at least at the speed of about 30 m/min relative to a smooth wall (16). In view of this result and the fact that the filtered fibre mat on the wire is not smooth it is quite possible that a turbulent boundary layer is maintained during drainage already when the suspension speed relative to the wire exceeds 20 m/min, as suggested by the similarity of the experimental results in Figs. 5.

In papermaking the shear stress imposed by the wire is precisely the force that orients fibres and breaks down flocs. If a turbulent boundary layer is created the shear field is no longer effectively coupled to the suspension to orient the fibres. Thus the fibre orientation anisotropy can no longer be increased by raising the suspension speed relative to the wire and it may even decrease when the suspension speed increases, as is evident in Figs. 1 b and c. In the fibre orientation model the increasing intensity of turbulence would explain the large values of the parameter δ needed to reproduce the experimental results.

The shear-induced turbulent boundary layer would also explain why paper formation deteriorates very rapidly if the suspension speed relative to the wire is raised sufficiently, since in that case flocculation is not inhibited. If, however, drainage rate is increased and the related hydrodynamic forces are enhanced, the coupling of the suspension to the wire improves. This is in fact another explanation for the increase in the fibre orientation anisotropy observed for enhanced drainage in Fig. 5 b. We also point out that high values of the tensile ratio (upto R_T = 5) have been reported for a gap former where water is removed very rapidly from the suspension (17).

In conclusion, it appears that disturbances in the suspension flow and eventually the onset of shear-induced turbulence explains the observed plateau in the tensile ratio R_T as a function of increasing suspension speed. If this is correct then there is a fundamental hydrodynamic mechanism that determines the maximum value of the fibre orientation anisotropy in paper.

4. SCALE OF THE SHEAR FIELD

We shall next consider what determines the scale of the orienting shear field during drainage. In section 2.3 we concluded that below the shear-induced plateau the laminar fibre orientation model is a reasonable approximation. The scale of the shear field is fixed by the parameter β of the model that tells how much a fibre is able to rotate in the shear field.

One could then imagine that β is directly proportional to the time t_z it takes for the other end of a fibre to land on the wire. The faster the fibres come down, the weaker the anisotropy of fibre orientations should be. This sounds quite reasonable. β should thus be inversely proportional to the drainage speed v_z, i.e. the speed of the suspension through the wire. This also follows from the application to the Fourdrinier case of the fibre orientation model derived by Ryti et. al (10) for the oblique sheet mould (cf. Eq. (12)). However, the experiments of Svensson and Österberg (3), Fig. 5 b, show that in reality drainage speed v_z has only a small effect on the fibre orientation anisotropy.

The order of magnitude of v_z can be estimated from the data supplied (3) for the rate of web formation during drainage. In case of the experiments shown in Fig. 5 b the paper web grows at the rate of approximately 60 g/m²s during the initial drainage phase and at a 5 to 10 slower rate during the rest of the drainage. Given the suspension consistency of 3 g/l it follows that the drainage speed is about v_z = 1.2 m/min initially and 0.2 m/min in the end. Same orders of magnitude also apply to the case of the FPPRI experiments. For the fine paper samples the slice opening was typically 26 mm, machine speed 60 m/min and jet to "wet line" distance 1.5 m, say; thus we can estimate that on the average $v_z = (26\ \mathrm{mm}/1.5\ \mathrm{m})\cdot 60\ \mathrm{m/min} = 1$ m/min.

It appears, therefore, that the average drainage speed v_z is about 0.5 to 1 m/min in the experiments shown in Figs. 5. The corresponding values of β can be calculated from from Eq. (15) to be roughly 1 to 2 min/m for all the experiments. However, the model predictions R_N in these figures (the dashed and solid lines) are calculated for β = 0.05 and 0.10 min/m. A more than 10-fold increase in the value of β would give unrealistically rapid rate of increase for the orientation index R_N as a function of the suspension speed v_s.

In fact, according to the results of Svensson and Österberg (3) in Fig. 5 b, the fibre orientation anisotropy slightly increases with drainage rate rather than decreases as the model would predict. The increase was found to occur on the top (felt) side of the paper. This is reasonable since about half of the paper web is formed during the rapid initial drainage phase and the wet suction boxes only affect the second drainage phase and thus the top side of paper.

In any case, we must conclude that on Fourdrinier machines drainage speeds are by far too small to affect the distribution of fibre orientations in paper significantly.

Instead of drainage, the time t_z available for individual fibres to rotate could be determined by the suspension speed v_s relative to wire. It would then follow that t_z, and therefore β, should be inversely proportional to v_s. This is supported by the studies of Trevelyan and Mason (7) who find that in low consistency sheared suspensions the period of rotation of stiff fibres is inversely proportional to the shear gradient. It is immediately clear, however, that the time scale of fibre rotations cannot determined by the suspension speed v_s since if this were the case (i.e. β = const./v_s) then fibre orientation could not be controlled by the suspension speed ($\beta \cdot v_s$ would be constant).

We are then led to propose that the parameter β of the model is in fact determined by fibre-to-fibre interactions. During drainage a fibre that is anchored at one end to the filtered fibre mat is not free to rotate. Instead, the fibre is entangled with other fibres sticking up from the mat. Even in the suspension phase fibres cannot, in general, rotate freely since at the papermaking consistencies the suspension usually contains flocs of various sizes.

Thus the parameter β of the model appears to be essentially a property of the pulp suspension. In other words, the scale of the shear field is determined by pulp properties and not by paper machine parameters, just as the similarity of Figs. 5 a-c suggests. There are then at least two ways pulp properties may affect fibre orientation. The degree to which individual fibres are able to rotate depends on the resistance to rotation imposed by other fibres, fibre fragments and fines. Also, the ability of a fibre to rotate in a given environment may depend on the properties of the fibre itself. Both of these possibilities may apply in the headbox and during drainage on the wire.

In the experiments made on the FPPRI pilot machine it was observed that especially for small suspension speeds v_s the wood-free fine paper samples were more oriented than the wood-containing samples. Above, in section 2.3, it was concluded that this has to do with the different jet fibre orientation in the two cases. We point out that even though the main body of the pulp was different in the two cases (cf. Appendix) the stained fibres were of unbleached softwood fine pulp in all the samples. Thus in the LWC pulp the stained fibres encounter more resistance to rotation than in the fine pulp. The lower freeness of the former (180 ml CSF vs. 400 to 580 ml CSF) and the stiff mechanical pulp fibres contained in it may well account for this.

It thus appears that the resistance individual fibres encounter when they rotate in the headbox slice must by and large explain the different fibre orientation anisotropy of the fine paper and the LWC base paper. Other authors have also argued that the rheological properties of the pulp suspension should determine the fibre orientation anisotropy obtained for a given jet-to-wire speed difference (18). The effect of the pulp properties on the jet fibre orientation was demonstrated experimentally by Wrist (12).

We have not considered in detail the the effect of the fibre-to-fibre interactions on the fibre orientation. It seems that one should abandon the simplified equation of motion (1) in order to obtain a realistic description of the fibre-to-fibre interactions. Even though this would certainly change the model predictions quantitatively we would expect that qualitatively the results would not differ from those of the simple elliptic model derived above for the case of laminar suspension flow.

5. SHAPE OF THE FIBRE ORIENTATION DISTRIBUTION

Above it was argued that behaviour of the tensile ratio of paper as a function of the speed difference between the suspension and the wire can be explained by a laminar, elliptic fibre orientation model, provided that the speed difference is not too large. In the latter case, flow disturbances and turbulence control the fibre orientation anisotropy. Also, it was concluded that in the first case fibre-to-fibre interactions determine the fibre orientation anisotropy.

In this final section we shall study the effect of fibre properties on the fibre orientation distribution. The significance of the properties of the fibres themselves to the fibre orientation anisotropy was studied experimentally using image analysis. For each sample (1000 to 2000 fibres measured on each side) we calculated the correlation of the direction cosine $\cos(2\phi)$ with fibre length and fibre curl (see Appendix for details).

We found no significant correlation between the direction cosine and fibre length. The correlation coefficient varies erratically between -0.05 and 0.05 on both sides of the fine and LWC base paper samples. Thus in a given paper sample there should be essentially no difference between the fibre orientation anisotropy of long fibres and short fibres. This has been also found in other investigations (19). It is still quite possible, however, that the distribution of fibre orientation changes if the average fibre length of the pulp is changed since that may affect the fibre-to-fibre interactions. This was not studied systematically.

On the other hand, the direction cosine has a significant negative correlation to fibre curl. The correlation coefficient decreases systematically as the suspension speed v_s increases, from $r \approx -0.1$ at $v_s = 0$ to $r \approx -0.15$ at $v_s = 20$ m/min and further to $r \approx -0.3$ at $v_s = 40$ m/min. No difference was found between the fine and LWC papers. Because of the large number of fibres measured in each case the values of $r \leq -0.1$ are statistically significant.

The effect of fibre curl on fibre orientation is consistent with the suggestion that the amount by which a fibre can rotate during the drainage phase is determined by the resistance generated by fibre-to-fibre interactions. In that case it is clear that flexible fibres will adjust to the oriented shear field by bending themselves whereas stiff fibres must rotate. According to our experimental results the bending leads to a weaker fibre orientation anisotropy than the stiff rotation.

We note that the correlation between fibre orientation and fibre curl may be slightly affected, but not entirely determined, by the fact that in the image analysis measurement an average direction for each fibre is determined (cf. Appendix). As a result, the orientation distribution of straight fibres has the tendency to appear more anisotropic than the distribution of curly fibres since in the latter case fibre direction cannot be determined accurately.

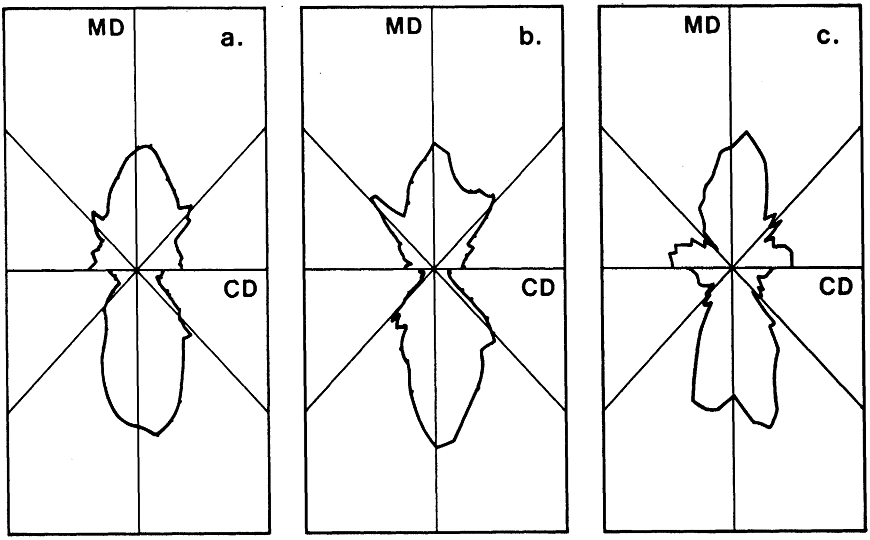

Fig. 7. Polar plot of the orientation distribution of the stained fibres in the MD-CD diagram with the top (felt) side pointing up and wire side down. The diagonal lines correspond to ±45° from the machine direction. FPPRI fine paper sample for v_S = 1 m/min with, a, all fibres visible on the paper surfaces included; b, only straight fibres; c, only curly fibres.

The importance of fibre curl is illustrated in Figs. 7-9 that correspond to the FPPRI fine paper samples at suspension speeds v_S = 1, 21 and 38 m/min, respectively. In the figures the polar plot of the orientation distribution of the stained fibres is in the MD-CD diagram with the top (felt) side pointing up and wire side down. The diagonal lines correspond to ±45° from the machine direction. The figures are all drawn to the same scale, so that they can be directly compared.

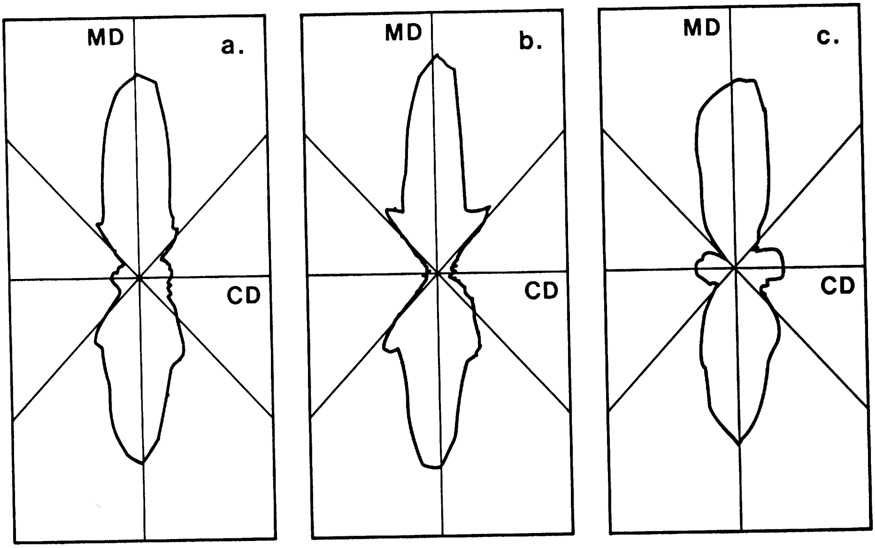

Fig. 8. As Fig. 7, the FPPRI fine paper sample for v_S = 21 m/min.

Included in Figs. 7-9 a are all the stained fibres visible on the paper surfaces, in Figs. 7-9 b only straight fibres, and in Figs. 7-9 c only curly fibres. The fibres were partitioned so that there are approximately equal numbers of straight and curly fibres in each case (cf. Appendix). It can be seen that curly and straight fibres have completely different orientation distributions. In the case of curly fibres there are minima at ±45° from the machine direction, whereas in the case of straight fibres there are local maxima at the same directions. The nonmonotonic behaviour of the fibre orientation distribution function as a function of the angle ϕ, though in weaker form, can be seen also in the overall distributions in Figs. 7-9 a.

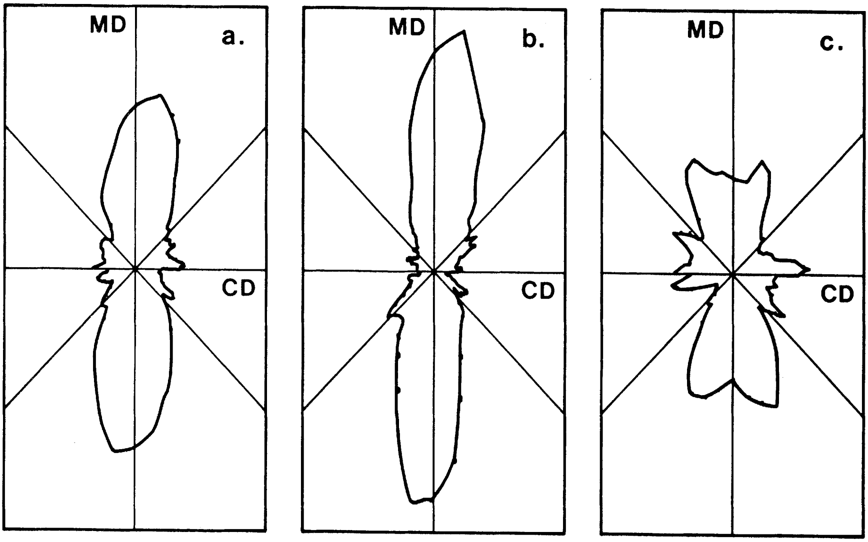

Fig. 9. As Fig. 7, the FPPRI fine paper sample for v_S = 38 m/min.

The unexpected local maxima in the fibre orientation distribution were observed already by Danielsen and Steenberg in 1947 (5), but no explanation for these "horns" was found. It seems to us that the "horns" or local maxima in the orientation distribution may in part correspond to fibres that land on the fibre mat "head" first. Fibres that land "tail" first rotate towards the machine direction, whereas fibres that land "head" first initially rotate away from it. The first fraction of fibres gives rise to the expected increase in the machine direction fibre orientation, but the latter fraction behaves differently. Some of these fibres remain oriented closer to the cross-machine direction than to the machine direction. These fibres could correspond to the local maxima in the orientation distribution.

In the model calculations, no local maxima occur in the elliptic or von Mises distribution functions (Eqs. (7) and (16)). Local maxima are obtained only if the jet fibre orientation is included in the model (Eq. (19)). If we assume that $g(\phi)$ is elliptic, relatively weak local maxima are obtained similar to those in the measured distributions in Figs. 7-9 a. The distributions in Figs. 7 b and c, on the other hand, cannot be reproduced unless we assume that the jet orientation distribution is of that kind.

Thus it seems that the "horns" of the fibre orientation distribution could thus be created by the combing action of the oriented shear during the drainage phase. The model calculations demonstrate also that even if no "horns" are present in the distribution of the jet the anisotropy of the jet definitely affects the appearance of the "horns" in paper.

Some of the nonmonotonic shape of the orientation distribution may also be generated directly in the headbox. This cannot, however, be done by the acceleration of the suspension flow in the headbox slice, since it turns all fibres towards the machine direction, none away from it. On the other hand, however, the deorienting effects at the lip (14) may lead to a complicated shape of the jet fibre orientation distribution. In this respect we note that in the FPPRI experiments the local maxima of the distribution become weaker as the suspension speed v_S increases (compare Figs. 7 b and c to Figs. 8 b and c). When the suspension speed is very large (Figs. 9) the orientation distribution of the curly fibres - but not of the straight fibres - seems to be affected by the turbulence of the suspension flow and more local maxima are generated.

In summary, the shape of the fibre orientation distribution, and the local maxima in particular, are probably in part caused by the headbox and in part by the oriented shear on the wire. The shape of the distribution appears to be very sensitive to the wet fibre flexibility.

6. CONCLUSIONS

We have analysed the physical mechanisms of fibre orientation in the Fourdrinier process by means of simplified model calculations. We suggest that in an oriented shear field the distribution of fibre orientations may be approximated by an elliptic distribution function as long as the suspension flow may be considered to be laminar. The elliptical model implies that the degree of fibre orientation anisotropy increases rapidly as the difference between the speed of the suspension (the jet) and that of the wire is raised.

Jet fibre orientation induced in the headbox is shown to lead to an approximately constant level of the machine to cross-direction tensile ratio R_T for a range of small speed differences. Since the jet orientation decreases during drainage its effects are more pronounced on the wire side of the paper made on a Fourdrinier. In the experiments on the FPPRI pilot machine the jet fibre orientation seems to lead to a considerable fibre orientation twosidedness in wood-free fine paper samples when the speed difference is small.

On Fourdrinier machines it is usually observed that the fibre orientation anisotropy can be increased by the oriented shear only up to a certain level. According to our analysis, the plateau in the tensile ration R_T appears to be caused by the onset of shear-induced turbulence. In the cases studied the plateau is reached at the suspension to wire speed difference of approximately 20 m/min independent of the speed of the paper machine.

In general the orienting effect of the shear field on the wire seems to be determined by fibre-to-fibre interactions, whereas paper machine parameters appear to be by and large irrelevant. It is observed that on the average stiff fibres are more anisotropically distributed than flexible fibres. The latter can adjust to the shear field by bending rather than just by rotating as the former have to do.

In summary, we have studied the basic physical mechanisms of fibre orientation. Even though the analysis has been strongly simplified the results should prove useful in assessing the significance of various factors on the fibre orientation anisotropy in paper. In particular, the effects of the headbox geometry, the twin-wire drainage and the pulp properties could be studied in more detail.

ACKNOWLEDGMENTS

We are grateful to many colleagues, H. Paulapuro and J. Koskimies in particular, for fruitful discussions and useful comments, for the pilot machine crew at the Institute for skillful preparation of the sample material, and for H. Eklund, K. Niemi and J. Virtanen for the image analysis measurements.

APPENDIX: EXPERIMENTAL PROCEDURES

Sample material

Paper samples were prepared on the FPPRI pilot machine of wire width 850 mm. This machine has rectifier roll headbox, Fourdrinier wire section, three nip press and 12 cylinder dryer, and a machine calender which, however, was not used. The wire section contains 6 foils, followed by 4 sets of a wet suction box and table rolls, and finally 6 dry suction boxes. In all experiments the jet speed was higher than or equal to the wire speed.

Wood-free and wood-containing paper was prepared using commercial pulp mixtures for fine paper, LWC base paper and newsprint. The wood-free paper was made of a fine paper mixture of softwood and hardwood bleached kraft pulp. Different freeness levels were used (400 to 560 ml CSF), but these were found to have no significance to the fibre orientation of the paper. The wood-containing paper was made of a 180 ml CSF LWC-pulp containing groundwood and bleached softwood kraft pulp and of a 110 ml CSF newsprint-mixture of bleached softwood kraft pulp, pressurised groundwood and thermomechanical pulp. Some paper machine parameters are given in Table 1.

Image analysis

About 0.3 % of stained fibres were added to the fine paper and LWC paper pulps for image analysis purposes. The stained fibres were of unbleached softwood kraft pulp in both cases. The stained fibre image of a sample is processed using an automatic image analyser (20) and various standard functions are

Pulp type	Fine paper	LWC	Newsprint
Basis weight, g/m^2	70	40	45
Machine speed, m/min	60	80	80
Lip opening, mm	26	28	26
Headbox consistency, %	0.27-0.41	0.19-0.23	0.25-0.30
MD draw, wire to reel, %	1.6	2.0	2.3
"Wet line" from headbox, m	1-1.5	3-4	2-4

Table 1. Paper machine parameters for the samples made on the FPPRI pilot machine.

evaluated for each individual fibre image. The orientation of a fibre is given by the orientation of the major axis of an ellipse that just covers the fibre image. Fibre length is determined by making the image repeatedly thinner until it is just one pixel wide. The average length of the fibre images varied slightly from sample to sample, between 1.5 and 2 mm, with the standard deviation around 1.5 mm.

Only the fibres on the surface of the sample are measured and thus separate results are obtained for the wire and felt side of the sample. The orientation distribution is weighted by the length of the image. This choice is arbitrary, but there exists no precise definition for the distribution of fibre orientations. The various alternatives are discussed by Mark and Perkins et al (21,22). We have checked that the orientation distribution would change only a little if all images were given the same weight. The measured fibre orientation distributions are quantified in terms of their first 2-3 Fourier coefficients, Eq. (10). We chose this approach since an arbitrary fibre orientation distribution can be accurately represented as an infinite Fourier expansion.

The curl index III of Jordan and Page (23) is used to quantify fibre curl

$$\text{curl III} = L/M - 1 \qquad (21)$$

where L is the length of the fibre image and M the length of the major axis of the covering ellipse. The median of the curl index of the stained fibres varied nonsystematically from 0.15 to 0.20 with the standard deviation around 0.1.

REFERENCES

1. For a review see e.g. Parker, J. D., S.T.A.P. #9, T.A.P.P.I., Atlanta (1972).

2. Schröder, S. and Svensson, O., Sv. Papperstdn. 68 (2), 25 (1965).

3. Svensson, O. and Österberg, L., Sv. Papperstdn. 68 (11), 403 (1965).

4. Htun, M. in: "Paper Structure and Properties", Bristow, J. A. and Kolseth, P., eds., Marcel Dekker Inc., New York, 227-240 (1986).

5. Danielsen, R. and Steenberg, B., Sv. Papperstdn. 50 (13), 301 (147).

6. Jeffery, G. B., Proc. Roy. Soc. A 102, 161 (1922).

7. Trevelyan, B. J. and Mason, S. G., J. Colloid Sci. 6, 354 (1951).

8. Perkins, R. W. and Mark, R. E. in: "The Role of Fundamental Research in Paper Making", J. Brander, ed., Mechanical Engineering Publ., Ltd., London, 479-526 (1983).

9. Rigdahl, M. and Hollmark, H. in: "Paper Structure and Properties", Bristow, J. A. and Kolseth, P., eds., Marcel Dekker Inc., New York, 241-266 (1986).

10. Ryti, N., Aaltonen, P., Perttilä, T and Talja, M., Paperi ja Puu, (3), 207 (1969).

11. Mardia, K. V., "Statistical Mechanics of Directional Data", Academic Press, New York (1972).

12. Wrist, P. E. in: "Formation and Structure of Paper", F. Bolam, ed., Tech. Sec. B.P.B.M.A., London, 839-888 (1962).

13. See e.g. Schulgasser, K., J. Mat. Sci., 20, 859 (1985).

14. Compare e.g. Papanastasiou, A. C., Proc. AIChE Mtg., Chicago, 10-16 Nov 1985.

15. Robertson, A. A. and Mason, S. G., "Formation and Structure of Paper", F. Bolam, ed., Tech. Sec. B.P.B.M.A., London, 791-827 (1962).

16. Robertson, A. A. and Mason, S. G., Tappi 40 (5), 326 (1957)

17. Wahren, D. and Lövstad, C., Das Papier 31 (10A), V132 (1977).

18. Plotnikov, I. A., Nepenin, V. N. and Kiprianov, A. I., Lesnoj Zh. (2), 72 (1986).

19. Rigdahl, M., Andersson, H., Westerlind, B. and Hollmark, H., Fibre Sci. Techn. 19, 127 (1983).

20. SEM-IPS, Kontron AG, West-Germany

21. Mark, R. E. in: "Handbook of Physical and Mechanical Testing of Paper and Paperboard", R. E. Mark, ed., Marcel Dekker, Inc., New York, vol 2, ch. 24 (1983).

22. Perkins, R. W., Mark, R. E., Silvy, J., Andersson, H. and Eusufzai, A. R. K., Proc. Int'l Paper Physics Conf., Harwichport, MA, 105-110 (1983).

23. Jordan, B. H. and Page, D. H. in: "The Role of Fundamental Research in Paper Making", J. Brander, ed., Mechanical Engineering Publ., Ltd., London, 745-766 (1983).

Transcription of Discussion

DISTRIBUTION OF FIBRE ORIENTATIONS IN PAPER

Dr. K. J. Niskanen, FPPRI

Dr. G.A. Baum, James River Corporation

Congratulations on a nice piece of work. It requires two polar angles to describe a fibre in suspension - one from the MD and one from the ZD I always felt that the angle from the ZD had an important part to play in the ability of a fibre to rotate into the MD. You did not really mention this except to talk about "noses" and "tails". Have you considered the z-direction orientation of the fibres in your analysis?

K.J. Niskanen

If you wanted orientation angle relative to the Z direction, I could put this in the Gamma constant, which contains all the nasty things. The other way to answer your question is that if I look at the exact equations of motion, there I do indeed have a coupling between the angle relative to Z direction and the angle relative to machine direction. However, those equations of motion are relatively complicated. If you do the equations, you have to assume that the velocity field is linear so that when you go away from the wire, the velocity of the suspension increases linearly. If I make this assumtion, then I find that the speed difference between suspension and wire has no effect on fibre orientation anisotropy and that is not what I really want. It is obvious that the time the fibres have available for rotation is determined by something other than the shear field, in other words, drainage is an important thing. If I take into account drainage forces, the hydrodynamics becomes very complicated.

Prof. B. Steenberg, Royal Institute of Technology

My question relates to the mathematical foundation of your definition of the direction of a fibre.

Your image analysis defines the direction of a fibre as the direction of the major axis of an ellipse in which the fibre can be circumscribed.

The direction of a point on a continuous curve is its tangent, while the direction of a curve from A to B is the integral of the direction of every point along the curve. This turns out to be the direction of a straight line from A to B. Curvature shows up by giving a distance from A to B shorter than the length of the curve. This holds also for the three dimensional case.

We know from polymer science that the relevant hydrodynamic property of a polymer is not its length (DP) or curvature but the distance and the direction between the two ends. Molecules like fibres are seldom straight.

Your image analysis includes curvature, which will define the axis of the ellipse. I do not believe the mathematical definition of the fibre direction is identical with your definition of direction.

K.J.Niskanen

In the model calculation all that is considered is straight sticks so the problem does not arise. In the image analysis case I do indeed use the direction of the longest axis of the ellipse to define the orientation of each fibre.

Prof B. Steenberg

Are the directions the same for the ellipse and the true direction of the fibre derived by integrating over the length of the fibre.

K.J.Niskanen

No in general they are not but the difference will depend on how you consider the fibre. For example, are you considering integration of the full fibre or segments of the fibre? I have not checked this in detail but it does not seem to make much difference.

Prof. B. Steenberg

In a continuous fibre the direction of one segment is not independent of the directions of the adjoining sections. So segment calculations are invalid, provided the fibre is not broken ("hinged"). Then the fibre is discontinuous and each part behaves more or less as a separate entity. My main point is that we must use well established definitions for direction when applying hydrodynamics. Somewhat surprisingly, curvature and flexibility do not play a role in a hydrodynamic context.

K.J. Niskanen

Actually it is all the same whether I used the fibre length which defined as going along the fibre or the longest axis of the ellipse. However I used it does not affect the measured orientation distribution, in other words there is no correlation between the length and the orientation of fibres.

Prof. B. Steenberg

Thank you. Next question. You are surprised that at zero difference in speed we do not get the expected tensile relation. When Danielsen and I ,in 1947, studied this we discovered one reason was the stretch in the paper machine. Whatever jet-wire relation we tried we could not get the required MD tensile value needed for twisting paper, like cable wrap, using a single felted Yankee machine. It could, however, easily be reached on MG machines with open draws, which of course required wet stretch.

We agree that wet stretch can hardly influence fibre orientation, but there is still a possibility which I pointed out in Montreal in 1949. Assume that my naked arms are two fibres and the hairs on my arms are fibrils on the fibre surfaces. If I cross my arms and move them over each other only slightly, the direction of my arms s hardly changed. But the movement will rapidly align and entangle the model fibrils in the contact area. This could explain the important strengthening effect of wet stretch.

K.J. Niskanen

It is quite obvious that stretch of the web will affect its mechanical properties and it is probable it will also affect the geometry of the network, about to this there can be no argument. You can never be quite sure when you look at tensile ratios if the minimum value is caused by orientation or by stretch or by both of them. Whilst admitting the affect of stretch you should not forget the affect which is caused by orientation that is created in the headbox; that is important.

B. Radvan B R Research and Consultancy Ltd.

Perhaps one reason that the orientation is not one at zero jet velocity difference is that there is no such thing as zero jet velocity difference! There is always an angle of impact effect, and there are differences in the speed of the jet throughout its depth.

M.B. Lyne International Paper USA

The difference between figures 8 and 9 in your text is an increase in the velocity of the stock. There is a difference in orientation angle top and bottom as you speed the jet up, such that on the top side there is a higher speed you have skew orientation to the right and on the wire side a skew orientation to the left. This could result in a complex curl problem, as you have pointed out. Since you are only sampling at one point on this narrow experimental paper machine does this difference in orientation angle top and bottom correspond to a flow vortex caused at higher jet velocity?

K.J. Niskanen

I would think that the orientation angle that you see in the image analysis results is more like an accident than systematic behaviour, in other words what we tried to do is take samples in the middle of the web. The web is something like 60cm wide and we know that the orientation angle is a fan like thing so that at the edges the angle points outwards or inwards depending on the jet to wire ratio.

M.B. Lyne

What explains the difference in orientation between the top and the wire side? By this I mean the angle in skew orientation.

K.J. Niskanen

I did not find this very surprising, after all we know that the speed of the suspension will slow down during filtration in such a way that it approaches the speed of the wire. In other words, the angle will move outwards. To be honest, I am not sure whether what we think to be machine direction is actually so. It may be out by a few degrees since the sample sheets are small.

Dr. Kari Ebeling, James River Corporation

There is a third mechanism which you should also take into account, the reflocculation of fibres in that part of the suspension which has not yet drained, especially on heavier basis weights, would this have an effect on your theoretical treatment?

K.J. Niskanen

This would have the effect that I cannot do it any more, I have left out all fibre to fibre interactions because they are so complicated to handle. The interesting aspect of your question is that if I want to fit my model with the maximum orientation ratio observed experimentally, then I have to assume that the flow directions vary from machine direction on average by 60 degrees, which is a huge angle. Therefore, it could be that instead of having individual fibres floating around, you could have flocs in which you cannot rotate the fibres, but they have a certain wide distribution of orientation angles. It also may be possible that the flocculation is induced by turbulence when the shear field becomes larger, but I have not looked to see if this fits the experiment.

Dr. J.F. Waterhouse, Institute of Paper Science & Technology

Cross flows may also have an important contribution. I have carried out some work recently using techniques developed by G. Baum and Habeger, former colleagues of mine using ultrasonic polar plots. In fact, we looked at paper made on a Fourdrinier paper machine with shake, and the lean angle which we calculate from the polar plot can change from the wire side to the felt side of the machine. We studied this by carrying out surface grinding of the sheet and studying the two sections. We have also seen examples that Bo Norman pointed out with the head box design that we can get significant cross flows from the head box obviously induced by the shake, which can lead to curl or off axis curl problems. Have you considered these CD flows in your analysis?

K.J. Niskanen

I have not actually worked on this, so am unable to comment.

B.D. Jordan, PAPRICAN

In contrast to Dr. Steenberg's position, we believe that the orientation distribution of fibre segments is more relevant to paper performance than is the orientation distribution of fibre end to end vectors.

For straight fibres, of course, the fibre orientation matches the segment orientation. In an oriented curly fibre,however, some segments will be oriented in other directions. One expects therefore, an isotropic contribution to the segment distribution in proportion to the curliness of the pulp. This was noted in Derek Page's review of the fibre curl in the previous symposium.

Some of the ambiguity in your results for curly fibres may be an artifact of your choice of a fibre orientation over a segment orientation distribution.

Moving to an end-to-end vector distribution would compound the ambiguity. A couple of simple examples will show this:
The letter U represents the shape of a fibre which would be oriented by flow in a direction normal to its end-to-end vector.

Also, we could take a circle o for which the segment orientation is zero, and break it into two semi-circles c > for which the net segment orientation remains zero, but in which the end-to-end vector is quite oriented. The same would continue if the semicircles are connected end-to-end: c>

On another matter, since the orientation of flocs is a separate problem from the orientation of single fibres, it would be interesting to note whether curly fibres are more likely to be found within flocs than by themselves.

K.J. Niskanen

In the image analysis measurements of the orientation of a fibre was the direction of the major axis of the covering ellipse. We observed that the curl of the fibre (eg. Curl index III of Jordan & Page, but also other curl indices), was correlated with the orientation of the fibre, ie. CD fibres were curly, MD fibres straight. I think this is due to the bending of the flexible fibres vs. rotation. In this sense, I think there is no ambiguity in the results for curly fibres.

I agree that the definition of orientation of curly fibres is not unambiguous. Experience has shown us that if the average orientation of a fibre is used, the distribution of fibre orientations agree with experimental observations of the tensile ratio or elastic ratio of paper. If one uses the distribution of segment orientation this is not the case - not at least for the paper samples we have studied. The situation could be different eg. for tissue paper.

Finally, I think it is a good idea to try and see if there are on the average more curly fibres in the flocs of paper than otherwise. It may be however, that our paper samples are not flocky enough for the flocs to be distinguished sufficiently well.